Jurnal Teknologi

Full Paper

INTEGRATING DEPOSITIONAL SYSTEM TRACTS WITH MINERALOGY AND PROVENANCE OF THE MIOCENE SANDSTONES, OFFSHORE NORTH KUTEI BASIN

Kuntadi Nugrahanto[a,b]*, Ildrem Syafri[a], Adjat Sudradjat[a], Budi Muljana[a]

[a]Postgraduate Program, Faculty of Geology Engineering, University Padjadjaran (UNPAD), Jl. Dipati Ukur 35, Bandung, West Java 40132, Indonesia
[b]Pertamina Hulu Energi Subholding Upstream (PHE SHU), PHE Tower, Jl. TB Simatupang Kav.99, Jakarta, Indonesia

Article history
Received
2 February 2023
Received in revised form
24 June 2023
Accepted
12 July 2023
Published Online
20 October 2023

*Corresponding Authors
kuntadi19001@mail.unpad.ac.id

Graphical abstract

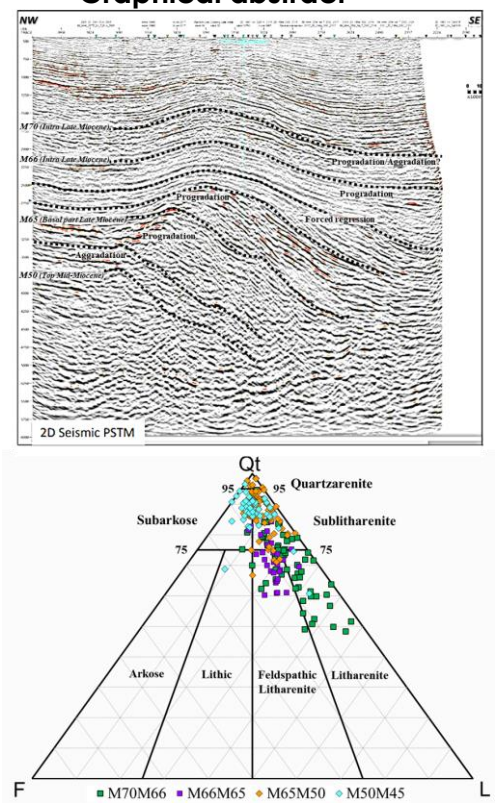

Abstract

Vertical variation of the Miocene sandstone mineralogy in the Kutei Basin has been recognized but the reasons for this remain unsaid. Deltaic-sandstone facies, parasequence sets, detrital mineralogy, and provenance of the uppermost Middle Miocene to the Upper Miocene strata in the Anamta and Amantu areas were analyzed using twenty-three wells and selected composite 2D and 3D seismic lines. Taxon indicators were correlated to build bio- and litho-stratigraphic markers: M50, M65, M66, and M70. The mineralogy dataset was derived from core and cuttings, while the detrital minerals were described, counted, normalized, and plotted in ternary diagrams. The four key markers were tied to the 3D-seismic data for seismic-stratigraphy analysis to observe the parasequences, system tracts, and sequence boundaries that correspond to the fluctuated relative sea-level. The parasequence sets are: (1) M65 aggradation and progradation, (2) M66 progradation, forced-regression, and back to another progradation, (3) M70 progradation, which interestingly demonstrate the detrital-mineral groupings. Qt-F-L suggests a gradual change up to the younger age from subarkose to sublitharenite towards feldspathic-litharenite to litharenite. Qp-Lv-Ls demonstrates the source was derived from collision-suture and folded-thrust belt. Qm-F-Lt diagram reveals the mature rocks with stable frameworks to the recycled-orogen provenance. The sediments maturity and stability are further confirmed by the Qm-P-K ternary chart. The most important finding is a significant shift of the paleo-shelf edge during the forced regression, as it separated the mineralogy composition of the M66 to the underlying M65 parasequence sets.

Keywords: Parasequence, system tracts, sandstones, detrital mineral, ternary diagram

1.0 INTRODUCTION

1.1 Background and Objectives

The focused study covers 1,300 (of ca.5,000) sq.km area at the northern offshore of the Kutei Basin situated between the Anamta and Amantu fields. The study area is bounded to the north by the main Anamta Field, to the east by the Ahsanta Field, to the south by the main Amantu Field, and to the west by the Atamba Field (Figure 1). There were relevant studies conducted in the offshore Kutei Basin that exclusively discussed the sequence stratigraphy in field-scale dimension: the Serang [1] and Sisi-Nubi [2] Fields, as well as the regional-scale studies of high-resolution sequence biostratigrapy [3 and 4], and regional depositional enviroment [5]. While there are other studies in the onshore Kutei Basin primarily examined the sandstones mineralogy and petrography of the Middle Miocene [6] and the Lower Miocene [7], and a more regional-scale QFL and lithofacies study [8]. However, none of these listed references yet to integrate both the sequence stratigraphy and the sandstones mineralogy to further understand the vertical changes of the mineralogy composition through the parasequences.

Integrating sequence stratigraphy with the other geological aspects; but not with the detrital minerals, have been applied in the last decade. The relationship between the fluctuation of relative sea-level and sedimentation rate of the siliciclastics package establishes the predictive capabilities for the reservoir-deliverability evolution across the sedimentary successions [9]. The coarse-grained gravity-flow sediment in turbidite system may potentially deposit significant amount of the organic-carbon materials [10]. Inline with these integrated studies, the objective of this study was to divide the overall progradation succession into parasequence sets to subdivide the detrital-mineral composition of the sandstones into unique groups. Analyzing the petrofacies and detailed compositions of detrital mineral on each parasequence sets were conducted to interpret the depositional settings and provenance along with the tectonic settings. Results of this study would enable us to deduce the history of Kutei Basin and provide more comprehensive understanding on the potential of the petroleum reservoir.

The existing biostratigraphy evaluation suggests the study interval comprises the uppermost of Middle Miocene to the lowermost of Upper Miocene. The study interval has a thickness range up to 700 m and consists of deltaic sandstones as the main hydrocarbon-producing reservoirs that intercalate with shale facies.

The stratigraphic sequence commences with more marine succession at the base and gradually changed into deltaic succession at the upper part, showing overall progradation parasequences at the onshore area [12] and as shown by the seismic data [5]. However, a detailed biostratigraphy study at one of the Anamta well [13] indicated there were dozens of transgressive and regressive repeated cycles. Interestingly, this study has observed that each stratigraphic sequence shows mineralogy variation of the sandstones. Detrital mineral of these sandstones are classified using the ternary diagram by Dickinson in 1985 [14]

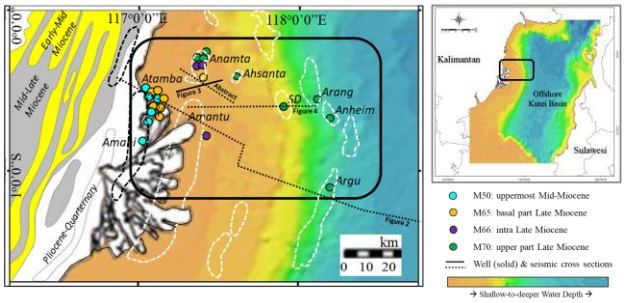

Figure 1 Basemap of the seismic lines with wells in varying-colored icons indicating the sample intervals. White-dotted polygons are field outlines, yellow-grey-white polygons on the left-hand side is simplified surficial geological map [11]

2.1 Geological Setting

The Cenozoic succession in the Kutei Basin consists of four main tectono-stratigraphic events: 1) Middle Eocene NE-SW [15] lineaments formed during the partial subduction along the Sundaland's edge due to the initiation of Australian continent to the north direction ca. 45 Ma [16]. This extensional trend is associated with the dominant terrestrial facies in the onshore lower Kutei to the marine succession in the offshore upper Kutei Basin. In addition to the NE-SW trend, a NW-SE basement-high trends are observed in the deep-water Kutei Basin, known as the North Makassar Basin [17, 18]. 2) Late Eocene to Oligocene basin sag filled with fine-grained materials of the marine facies in the embayment [16] might be associated with the ~35° counterclockwise (CCW) block rotation [19]. When the sagging ceased by the Late Oligocene back-stepping carbonate reefs that took place and developed over the flexural highs at the northern and southern boundaries of the Kutei Basin [20].

3) Early Miocene contraction had triggered a massive clastics progradation over the proto-Mahakam delta to the east, which was interpreted to be associated with the additional ~10° CCW Borneo rotation [19]. The Kutei's deltaic progradation reached its highest sedimentation rate in the Middle Miocene, known Middle Miocene Unconformity / MMU [21] with 14, 11, 8.5, and 3 Ma the main phases of uplift [4]. This huge sedimentary mass had initiated gravitational gliding with toe-thrust fold belts at the distal area [22]. 4) Pliocene compression had formed the N-S Samarinda anticlinorium [23] and prevented the sediment transport from the highlands to pass the anticlinorium, hence the Kutei Lake was formed. A significant volume of sediment was still able to flow along the course of the proto-Mahakam River [24].

2.0 METHODOLOGY

This study utilized various resources to observe the vertical and lateral facies variation, which included but were not limited to the Pertamina Hulu Energi Subholding Upstream (PHE SHU)'s wellbores, 3D-seismic reflection data, and exclusive reports as well as related published articles. The seismic reflection is derived from sound-wave transmission propagated down into the earth and reflected to the surface when it comes across different rock densities [25]. The reflection is recorded and displayed as two-way travel time in milliseconds unit.

The evaluation of cyclicity patterns in assessing the depositional cycles has been established in Vietnam, Indonesia, and Malaysia (VIM) called Sequence Biostratigraphy method, where several key cycles are applicable throughout the major sedimentary basins in the Sundaland, including the Kutei Basin [26]. In modification to the 2003's internal biostratigraphy study, six taxon indicators (Table 1) were recognized in providing datum age for well and seismic correlation markers of "M" [5] and "KR" [3] throughout the study area.

Table 1 Key-correlative markers [3, 5] referred to the datum age based on taxon indicators and their system tracts

"M" Marker	"KR" Marker	Datum Age	NN Zonation	Taxon Indicators and marker character
M70	KR70	7.0 Ma	Top NN11B	Top *Discoaster loeblichi* : DL5 maximum flood
	KR90	8.7 Ma	Intra NN10B	Top *Discoaster prepentaradiatus* : top in DPP1 maximum flood
M66		9.0 Ma	NN10A	Top *Discoaster bollii* : top in DPP1 maximum flood
M65	KR100	10.43 Ma	Intra NN9	Base *Catinaster calyculus*: base within DH2 lowstand
M50		11.29 Ma	Base NN8	Base *Catinaster coalitus*: condensed section
M70		11.3 Ma	Top NN7	Top *Discoaster deflandrei*: intra DH1 lowstand

The application of sequence biostratigraphy extended its applicability to help sharpen the relationship between sedimentation rates to the deformation cyclicity in the basins along the circum-Borneo [4, 21]. In line with it, Figure 2 describes an overall progradation parasequence in the northern offshore Kutei Basin [3] comprising a series of the highstand system tract (HST) bounded by conformable and unconformable strata. The lower-right illustration in the Figure 2 explains the highstand (HST), transgressive (TST), and lowstand (LST) system tracts, which were described based on the parasequence-set controlled by the seismic geometry and facies affiliated to the system tracts [27].

The selected 211 deltaic to deep-water sandstone samples of the M50 up to the M70 interval were utilized to classify the petrographic analysis on a total-quartz basis. 75 samples of them were further analyzed using mono and polycrystalline quartz. All samples were mostly taken from conventional-core plugs and side-wall cores. In addition to those, the study included the fifteen newly acquired rock-cutting samples at one of the recent Amantu wells, and nine additional core chips from one of the deepest wells at the Anamta field.

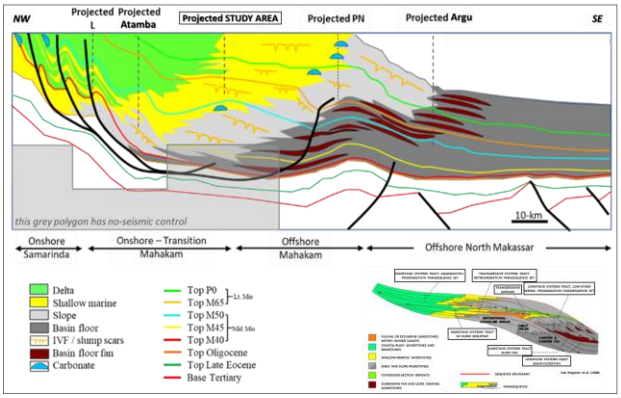

Figure 2 NW-SE Offshore Kutei (=Mahakam) section demonstrating the aggradation-progradational parasequence sets; modified from [5]

Pertamina Hulu Kalimantan Timur (PHKT) had conducted most of the thin-section petrographic analysis of the core-plug and rock-cutting samples, while Laboratory of Petrology – Mineralogy of *Fakultas Teknik Geologi Universitas Padjadjaran* (FTG Unpad) described the core-chip samples. These became the primary dataset in this study to define the trends of mineralogy grouping in separate system tracts. The detrital mineral compositions were quantitatively determined using modal analysis on thin slices of rock samples pasted on glass slides under the optical microscope. The different minerals were petrographically described and point-counted in 400 grid points and showing their proportion in relative abundance. The detrital components of total quartz grain (Qt), mono and polycrystalline quartz grains (Qm and Qp), feldspar (F), lithics (L), and total lithics (Lt) were normalized to 100 percent with reference to the Dickinson's classification, 1985 [14].

The detrital-mineral variety of sandstones in this study was plotted in ternary diagram introduced by Dickinson in 1985 [14], and they were normalized to 100% total amount of the total quartz, feldspar, and lithics (Qt-F-L), polycrystalline quartz, volcanics-derived lithics, and sedimentary-rock derived lithics (Qp-Lv-Ls), mono-crystalline quartz, feldspar, and total lithics (Qm-F-Lt), monocrystalline quartz, plagioclase, and K-feldspar (Qm-P-K). These percentages were plotted in the ternary diagram suggesting the tectonic setting of sedimentary provenance [14]. The normalized numbers of Qp were positioned at the Lt's pole in the Qm-F-Lt ternary diagram; and at the Qt's pole in the Qt-F-L ternary diagram. Since cherts are sedimentary rocks in origin, they were plotted at the rock fragment's pole of the ternary plot, while the F pole accommodates every type of feldspar grains including those with granitic source. The tectonic setting, provenance, and source-rock composition of sandstones in the study

interval were summarized in the format of modal-data analysis plotted in ternary diagrams in reference to Dickinson, 1985 [14]. Summary of methodological sequence in this study is shown in the Figure 3.

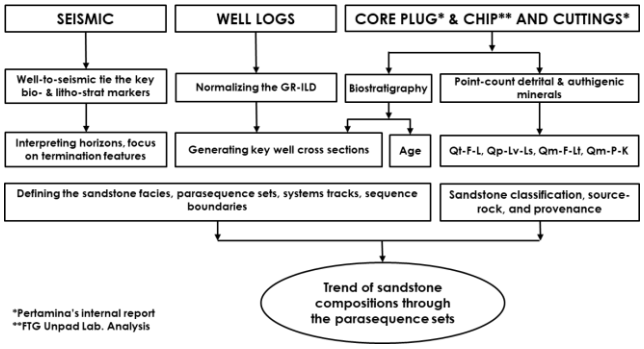

Figure 3 Three main datasets: seismic, well logs, rocks (core and cuttings) samples as the basis of overall methodological sequence of this study

3.0 RESULTS AND DISCUSSION

Datum age derived from taxon indicators was utilized to compile the existing field-scale markers across the study area to be classified into four integrated biostratigraphy markers: M50, M65, M66, and M70 [3]. These markers were carefully tied to the seismic data for seismic-stratigraphy analysis throughout the study area with no-well penetration. Identification of major sequence boundaries as its response to relative sea-level drop was found to be important in this research for providing the third order (seismically) and fourth order (well-based) sequence boundaries so called forced regression [28].

Both proven and interpreted M50's equivalent-age incised valleys that represented by thickly bedded channel sandstones were very well documented at the Pertamina Hulu Sanga Sanga (PHSS) acreage onshore Kutei Basin. These deep incision features (>100-feet) were identified in 3D seismic and wells with core data as the LST parasequence [5]. Seismic-driven slump-scar features associated with the lowest eustatic level were indicated along the Tunu anticline. These slump scars are equivalent in age with the M65 marker [5]. Up in the younger age of M70 equivalent, there was core data recovering ca.60-feet fluvial-channel sandstones that overlain and underlain by open-marine shales [5]. Multiple LST events across these different intervals had enabled the shelf to be shifted distally with incisions carving the by-passed shelf to provide passages in delivering proximal and coarser clastic sediments further onto the deeper water depositional system.

Dip-line wellbore cross section (Figure 4) indicated fourth-order flooding surfaces of 6a to 5a (near M65) markers, which are correlated to Intra NN-9 (Late Miocene). These flooding surfaces represent the high-GR shale separating the up-ward coarsening packages called sub parasequences; and tied them to the seismic data.

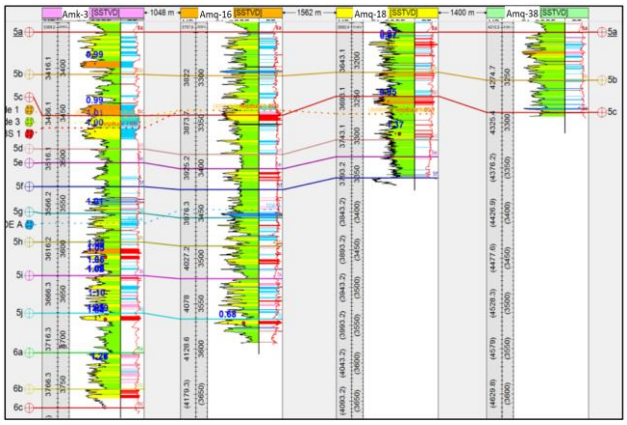

Figure 4 W-E orientation (dip line) wellbore cross section marking the fourth-order flooding surfaces in the northern part of the Amantu Field

Dip-direction composite seismic lines in the study area near Amantu and Anamta Fields had observed aggradational and progradational parasequence sets from the M50 to M66 regional markers. These composite seismic lines had clearly identified an overall progradation succession from west to east and from M50-to-M70 intervals, vertically (Figure 5) These parasequence sets can be further defined into four HST and one LST system tracts whereas the HST-01 and 02 are in the M65-M50 interval, while the HST-03, LST-01 (LSW), and HST-04 are in the M66-M65 interval (Figure 5).

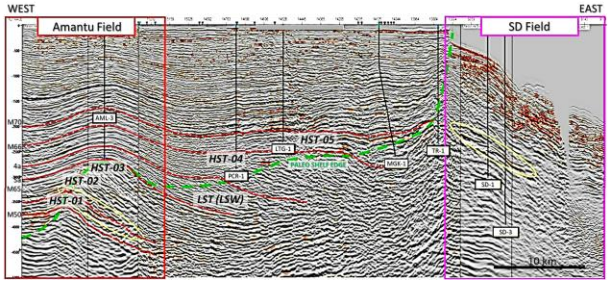

Figure 5 W-E orientation composite seismic lines represent a dip regional line showing depositional system tracts. Left-hand side yellow polygon shows the basal part of Upper Miocene's (M65) paleo deep-water slope, while the right one is the upper part of Upper Miocene's (M70)

Seismically, the paleo-shelf edge during the HST-01 and HST-02 systems tract shows aggradation and is slightly prograded to the east, respectively. The paleo-shelf edge at the HST-03 systems tract further prograded towards the east before it significantly shifted during the low-stand system tract (LST) forming the low-stand wedge (LSW) because of forced regression due to substantial relative mean sea-level drop.

The mineralogical study demonstrated that the sandstones in the study area (Table 1) are dominant in quartz (blue bar) with various trends of the lithics (green bar) and minor feldspar (dark-brown bar) components. The average composition of detrital minerals of sandstones towards the younger age ranges from 87-70% quartz, 6-7% feldspar, and 7-23% lithics.

Table 1 Normalized average numbers of the Mid-to-Upper Miocene sandstone's detrital minerals based on total quartz with the bar-graph illustration

Markers equivalent			Normalized average numbers			
NN	M-markers	KR-markers	Q	F	L	n
NN11	M70M66	KR70-80	0,70	0,07	0,23	66
NN9-NN10	M66M65	KR90	0,82	0,05	0,12	16
NN8-NN9	M65M50	KR100	0,87	0,04	0,09	83
NN6-NN7	M50M45	KR120	0,87	0,06	0,07	46

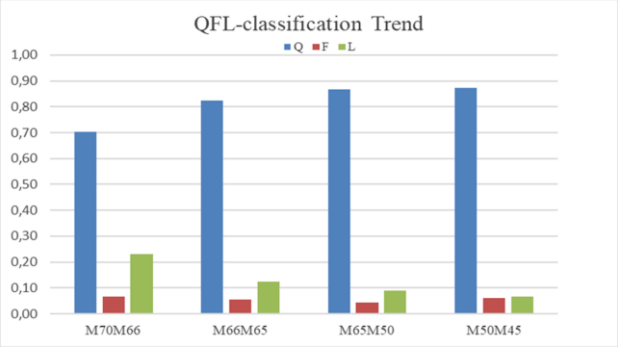

Sandstones petrographic analyses of the detrital and authigenic minerals, and point-counting exercise the QFL compositions of the Early-to-Late Miocene sandstones in Kutei Basin, Indonesia [6, 7, 8], the Tukau Formation in Sarawak, Malaysia [29], Paleozoic Sandstones in SW Sinai, Egypt [30], and the Qt, Qm, F, L and Lt of the Sawa Sandstones in SE Rajasthan, India [14] were able to define tectonic-related provenance and detrital-mineral composition of the sandstones. These studies are immensely helpful to discuss and summarize the sandstones classification with their tectonic settings. Their relationship is reflected in the ternary diagram to discriminate the origin and tectonic reconstruction of various terrigenous deposits.

In this study, the ternary diagram refers to Folk classification [14] shows that the composition of sandstones from M50 towards the younger age M70 graddually changes; in which quartzarenite, sub-litharenite to subarkose are substituted by feldspathic litharenite and litharenite (see the graphical abstract and Figure 6). The early Miocene (M40-M33) and basal part Middle Miocene (M45-M40) sandstones mineralogy at onshore wells varies from sub-litharenite to litharenite with dominant lithics content of metamorphic to sedimentary fragments [6, 7, 8].

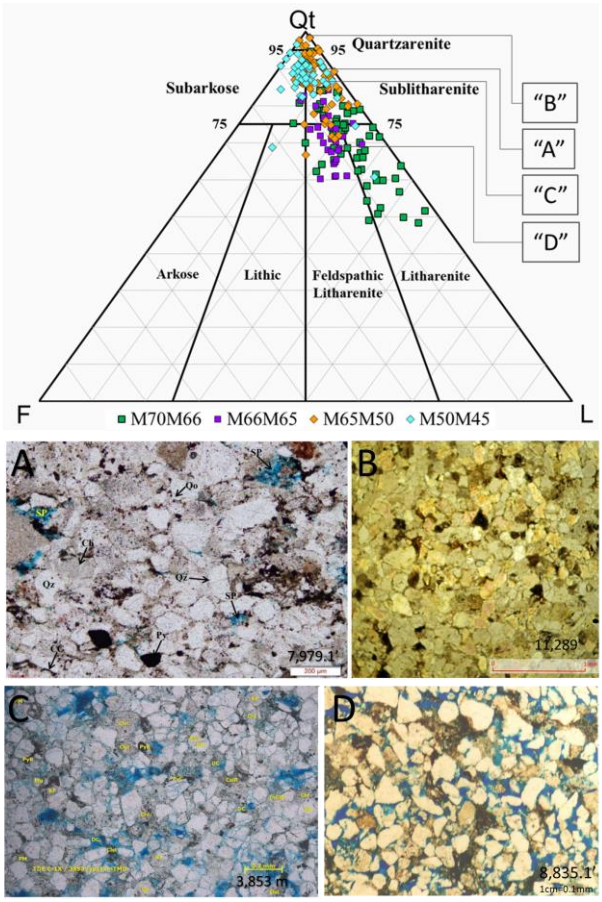

Figure 6 Photomicrographs of sandstones forming minerals from old to younger age as shown in the ternary diagram are: A. M50 sub-litharenite (Atamba-S44 core plug @7,979.1 ft), B. M65 quartz arenite (Anamta-O1 core chips @11,289 ft), C. M66 sub-litharenite (Amantu-C1 cuttings @3,853 m), D. M70 feldspathic litharenite (Ahsanta-8 core plug @8,835.1 ft)

The whole quartzose grains were put in the Qt's pole at the Qt-F-L ternary diagram (Figure 7) with the purpose of characterizing the detrital-grain establishment, source rock, provenance, weathering process, the transportation systems. The Qt-F-L diagram in this study is referred to Dickinson, 1985 [14] and suggested the samples are recycled-orogen provenance, where a small part of the older-rock samples in the M50-M45 and M65-M50 indicated that the continental-block provenance with sources of the stable craton. The rest of younger rock samples from the M65 to M70 are sequentially increasing in the ratio of oceanic-to-continental materials (Figure 7).

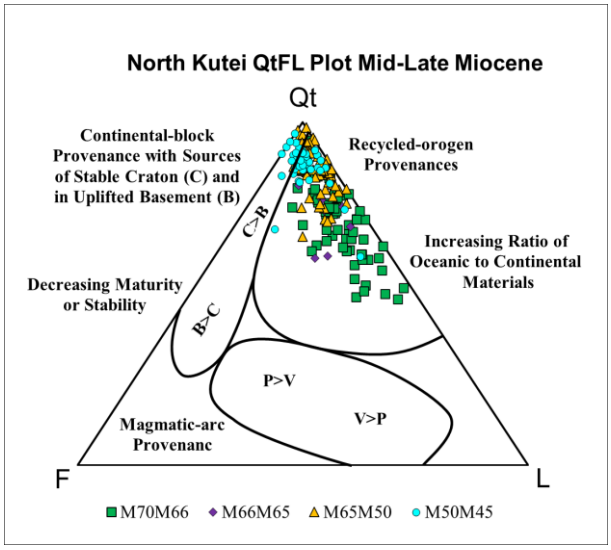

Figure 7 Qt-F-L ternary diagram of the Middle-to-Late Miocene samples in reference to Dickinson, 1985 [14]. Notes: Qt, F, and L compositions are in Table 1

Unavailable description of the monocrystalline quartz in the Middle Miocene (M50) to basal part of Upper Miocene (M65) sandstone samples at the Atamba and Amani wellbores had induced this study to commence mineralogical description of nine core chips solely from the Anamta-O1 wellbore, one of the deepest well in the Anamta Field. Since the M50 rock samples are no longer incorporated, further modal analysis will specifically discuss the Upper Miocene sandstone samples. The Qm-F-Lt modal analysis presents the average composition of detrital minerals from the M65 sandstones up to the younger intervals vary from 38 to 62% monocrystalline quartz (blue bar), 15 to 9% feldspar (dark-brown bar), and 47 to 29% total lithics (green bar, Table 2).

Table 2 Normalized average numbers of the Upper Miocene sandstone's detrital minerals involving the monocrystalline quartz Qm-F-Lt with bar-graph illustration

Markers equivalent			Normalized average numbers			
NN	M-markers	Palynova	Qm	F	Lt	n
NN11	M70M66	KR70-80	0,62	0,09	0,29	56
NN9-NN10	M66M65	KR90	0,83	0,06	0,11	19
NN8-NN9	M65M50	KR100	0,38	0,15	0,47	9

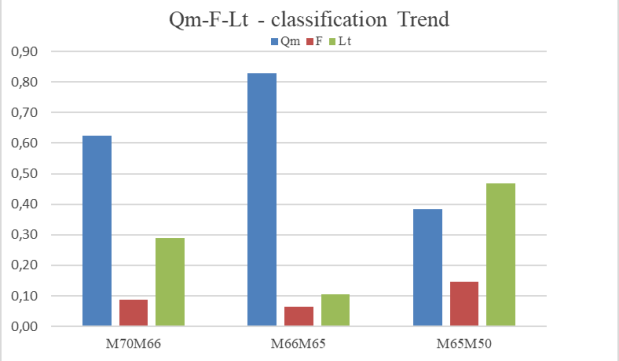

With the purpose of making observation on the rock provenances, the total rock fragments (total lithics) described in the rock samples were plotted in the Lt's pole at the Qm-F-Lt ternary diagram. The ternary plot shows that the samples range from the mature rocks with stable frameworks to the recycled-orogen provenance (Figure 8).

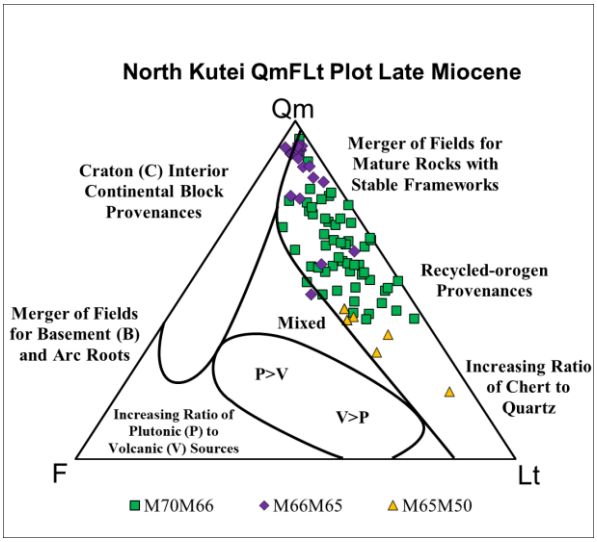

Figure 8 Qm-F-Lt ternary plot of the Late Miocene sandstone samples refers to Dickinson, 1985 [14]. Notes: Qm, F, and Lt compositions are in Table 2

The sandstone mineralogical analysis of Qp-Lv-Ls indicated that the normalized average composition of detrital minerals up to the younger age vary from 79 to 28% polycrystalline quartz (blue bar), none to 10% volcanic-derived lithics (dark-brown bar), and 21 to 62% sedimentary-rock-derived lithics (green bar, Table 3).

Table 3 Normalized average numbers of the Late Miocene sandstone's detrital minerals involving the polycrystalline quartz Qp-Lv-Ls with the associated bar graphs

Markers equivalent			Normalized average numbers			
NN	M-markers	Palynova	Qp	Lv	Ls	n
NN11	M70M66	KR70-80	0,28	0,10	0,62	54
NN9-NN10	M66M65	KR90	0,29	0,08	0,64	12
NN8-NN9	M65M50	KR100	0,79	0,00	0,21	9

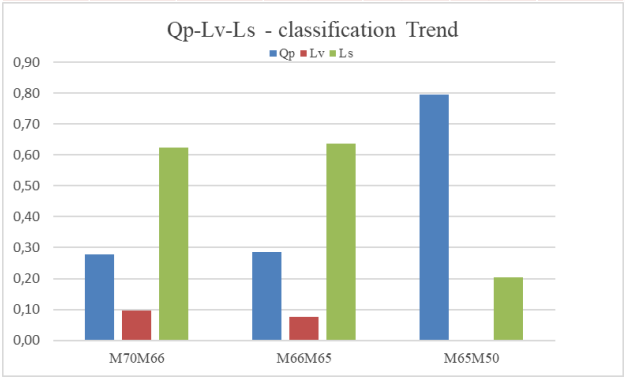

A more detailed characterization is clearly defined in the Qp-Lv-Ls ternary diagram (Figure 9), where the source of Upper Miocene rock samples is derived from the collision-suture and folded-thrust belt.

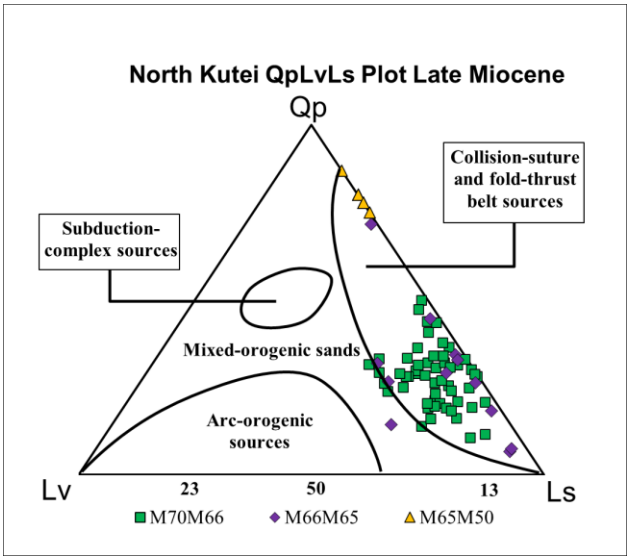

Figure 9 Qp-Lv-Ls ternary plot of the Upper Miocene sandstone samples referred to Dickinson, 1985 [14]. Notes: Qp, Lv, and Ls compositions are in Table 3

The Qm-P-K modal analysis shows that the normalized average composition of detrital minerals from the M65 sandstones up towards the younger age vary from 73 to 88% monocrystalline quartz (blue bar), 9 to 10% plagioclase (dark-brown bar), and 18 to 2% K-feldspar (green bar, Table 4).

The Qm-P-K ternary plot of the rock samples (Figure 10) demonstrates that the sediments were derived from the continental block provenance suggesting the maturity of the sedimentary rocks with stable framework.

Table 4 Normalized average numbers of the Upper Miocene sandstone's detrital minerals involving the monocrystalline quartz Qm-P-K with the associated bar-graph illustration

Markers equivalent			Normalized average numbers			
NN	M-markers	Palynova	Qm	P	K	n
NN11	M70M66	KR70-80	0,88	0,10	0,02	54
NN9-NN10	M66M65	KR90	0,91	0,06	0,02	12
NN8-NN9	M65M50	KR100	0,73	0,09	0,18	9

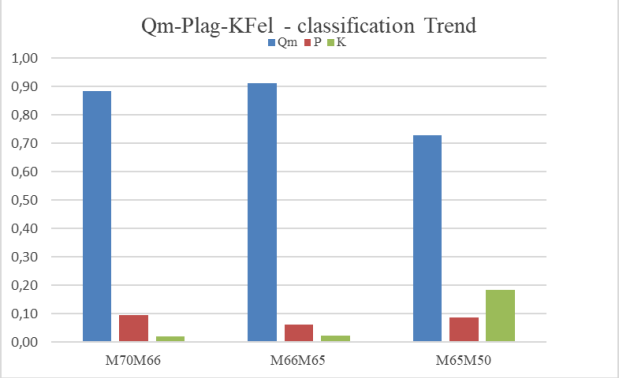

The last three ternary plots interestingly show the older rock samples (M65-M50) always stand out separately from the group of younger rock samples. Utilizing total quartzose grains (Qt), the ternary diagrams show a gradual trend on two aspects from the older to younger-age rock samples, which sequentially represent the HST-01, HST-02 up to the HST-05 system tracts, respectively: (1) from litharenite to sub-litharenite toward feldspathic litharenite to litharenite, and (2) from the continental-block towards the recycled-orogen provenances.

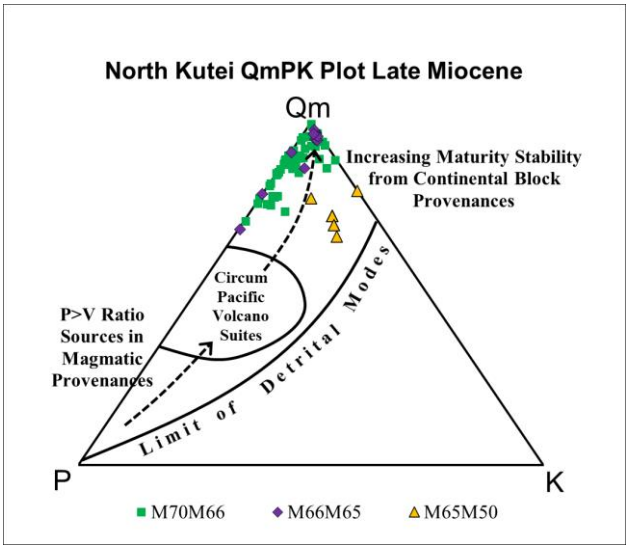

Figure 10 Qm-P-K ternary plot of the Upper Miocene sandstone samples referred to the Dickinson's classification, 1985 [14]. Notes: Qm, P, and K compositions are in Table 4

However, when the total quartzose grains were further classified into mono and poly-crystalline quartz in the ternary plots, the samples from the M65-M50 that represent the HST-01 and HST-02 sit distinctly from the younger-age rock samples.

4.0 CONCLUSIONS

An important finding in this study is the massive shifting of the paleo-shelf edge further east indicated by the LST (forced regression). This significant shifting had subdivided the M65 from the M66 intervals. This separation is clearly perceived by the mineralogy, sandstone classification, source provenance, and its maturity.

According to the integrated wellbore correlation and seismic interpretation, this study has identified at least seven depositional system tracts (Table 5). The lowermost system tract of M65 is subdivided into two systems tracts: aggrading HST-01 and prograding HST-02. The sandstone mineralogy is composed of quartzarenite to sub-litharenite as recycled-orogen product from collided suture and folded-thrust.

Table 5 Summary table of the depositional system tracts subdividing the Middle-Upper Miocene sandstone classifications based on the modal analyses using ternary diagram of detrital minerals in the study area

Datum age (Ma)	"M" Marker	System tract	Parasequence set	Sandstone Classification*	Qt-F-L Classification**	Qm-F-Lt Classification**	Qp-Lv-Ls Classification**	Qm-P-K Classification**
7.0	M70	HST 05	Progradation / Aggradation	Sublitharenite, Litharenite	Recycled-orogen Provenance; more Oceanic materials	Recycled-orogen Provenance; mature and stable rock frameworks	Collided suture and folded-thrust belt sources with more sedimentary rock fragments	Continental Block Provenance with increasing maturity and stability
9.0	M66	HST 04	Progradation	Sublitharenite, Feldspathic-litharenite	Recycled-orogen Provenance; more Continental materials	Recycled-orogen Provenance; mature and stable rock frameworks	Collided suture and folded-thrust belt sources with more sedimentary rock fragments	Continental Block Provenance with increasing maturity and stability
		LST (LSW)	Forced regression					
		HST 03	Progradation					
SHELF-EDGE SHIFTING FURTHER EAST								
10.4	M65	HST 02	Progradation	Quartzarenite, Sublitharenite	Recycled-orogen Provenance; more Continental materials, source of stable craton	Recycled-orogen Provenance; less mature with more Chert:Quartz ratio	Collided suture and folded-thrust belt sources with much less rock fragments	Continental Block Provenance with less maturity and stability than the younger rocks
		HST 01	Aggradation					
11.3	M50	HST 00	Progradation	Quartzarenite, Subarkose, Sublitharenite	Recycled-orogen Provenance; more Continental materials, source of stable craton	N/A	N/A	N/A

*[14, 29, 30]
**[14]

The overlying M66 is subdivided into three system tracts, which initiated the shelf-edge shifting to the east. The sandstones in this interval are classified as sublitharenite to feldspathic litharenite as the result of recycled orogen from collided suture and folded-thrust-belt sources. Hence, the sandstones are determined to contain more lithics, more mature, and more stable frameworks than the M65 rock samples.

Conflicts of Interest

The author(s) declare(s) that there is no conflict of interest regarding the publication of this paper.

Acknowledgements

Special acknowledgements to the Pertamina Hulu Energi Subholding Upstream (PHE SHU) and Postgraduate Program Faculty of Geology Engineering, University Padjadjaran (UNPAD), who had been fully supportive to this research. Further acknowledgement is given to the Centre of Data and Information Technology (Pusdatin) of the Ministry of Energy and Mineral Resources (ESDM), the Republic of Indonesia for the data permission and accessibility.

References

[1] Handoyo, K. 2003. Sequence Stratigraphy and Reservoir Heterogeneity of the Serang Field, Kutei Basin, Indonesia, Thesis Degree of Master of Science (Geology). Faculty and the Board of Trustees of the Colorado School of Mines.

[2] Cibaj, I., Ashari, U., Dal, Jacques-Antoine, Mazingue, V., Bueno, M. 2015. Sedimentology and Stratigraphic Stacking Patterns of The Sisi-Nubi Field Producing Interval, Lower Kutei Basin, East Kalimantan, Indonesia, *Proceedings Indonesian Petroleum Association 39th Annual Convention and Exhibition*, May 2015.

[3] Morley, J. M., Decker, J., Morley, H. P., Smith, S. 2006. Development of High Resolution Biostratigraphic Framework for Kutei Basin. *Proceedings, Jakarta 2006 International Geosciences Conference and Exhibition*, August 2006. https://doi.org/10.33332/jgsm.geologi.v22i1.574.

[4] Morley, J. M. 2014. Rifting and Mountain Building Across Sundaland, a Palyno-logical and Sequence Biostratigraphic Perspective. *Proceedings Indonesian Petroleum Association 38th Annual Convention and Exhibition,* May 2014.

[5] Nugrahanto, K., Syafri, I., Muljana, B. 2021. Depositional Environment of Deep-water Fan Facies: A Case Study of the Middle Miocene Interval at the Kutei and North Makassar Basins. *Journal of Geology and Mineral Resources*. 22(1): 45-57. https://doi.org/10.33332/jgsm.geologi.v22i1.574.

[6] Aryati, F. D., Setiawan, T., Meilany, Y., Assalam, A. 2019. The Progressive Illitization Process, Diagenetic Mechanism and Its Effect on Reservoir Quality based on SEM, Burial History, and Simultaneous Multi-well Analysis: A Case Study in the Sanga-sanga Block, Kutai Basin, East Kalimantan. *Proceedings Indonesian Petroleum Association 43rd Annual Convention and Exhibition*, October 2019. https://doi.org/10.29118/IPA19.SG.45.

[7] Werdaya, A., Alexandra, M., Nugrahanto, K., Anshori, R., Pradipta, A., Armitage, P. 2017. Comprehensive Evaluation of Reservoir Quality in the Early Miocene, Kutei Basin, Onshore East Kalimantan. *Proceedings Indonesian Petroleum Association 41st Annual Convention and Exhibition*, May 2017.

[8] Nugrahanto, K., Syafri, I., Muljana, B. 2021. QFL and Litho Facies: Predicting Reservoir Quality of the Middle Miocene Deep-water Facies at Kutei and North Makassar Basins. *Bulletin of the Marine Geology*. 36(1): 1-14. https://doi.org/10.32693/bomg.36.1.2021.706.

[9] Morad, S., Ketzer, J. M., De Ros, L. F. 2013. Linking Diagenesis to Sequence Stratigraphy: An Integrated Tool for Understanding and Predicting Reservoir Quality Distribution. *International Association of Sedimentologists, Special Publication (2012)*. 45:1-36. https://doi.org/10.1002/9781118485347.

[10] Hussain, A., Al-Ramadan, K. 2022. Organic Matter Burial in Deep-Sea Fans: A Depositional Process-based

Perspective. *Journal of Marine Science and Engineering*. 10(5): 682. https://doi.org/10.3390/jmse10050682.
[11] Supriatna., S., Sukardi, and Rustandi, E. 1995. Geological Map of Samarinda Sheet, 1:250,000. *Geological Research and Development Center*, Bandung, Indonesia.
[12] Sunardi, E., Isnaniawardhani, V., Amiruddin, Haryanto, I., 2014. The Lithological Succession in East Kutai Basin, East Kalimantan, Indonesia: Revisited in a New Data on Litho-Biostratigraphic. *International Journal of Science and Research (IJSR)*.
[13] Morley, R. J., and Morley, H. P. 2010. Neogene Climate History of the Makassar Straits, with Emphasis on the Attaka Region, East Kalimantan, Indonesia. *Proceedings Indonesian Petroleum Association 34th Annual Convention and Exhibition,* May 2010.
[14] Mathur, J., Khan, A., Islam, M. 2016. Provenance, Petrofacies, Tectonic Setting and Diagenesis of Sawa Sandstones, Lower Vindhyan, in and around Rithola Village, Chittaurgarh, SE Rajasthan, India. *International Journal of New Technology and Research (IJNTR)*. 2(11): 54-59.
[15] Bachtiar, A., Purnama, Y. S., Suandhi, P. A., Krisyunianto, A., Rozalli, M., Nugroho, D. H. H., and Suleiman, A. 2013. The Tertiary Paleogeography of the Kutai Basin and Its Unexplored Hydrocarbon Plays. *Proceedings Indonesian Petroleum Association 37th Annual Convention and Exhibition,* May 2013.
[16] Hall, R. 2013. The Palaeogeography of Sundaland and Wallacea Since the Late Jurassic, *J. Limnology*. 72(s2). https://doi.org/10.4081/jlimnol.2013.s2.e1.
[17] Nur'Aini, S., Hall, R., and Elders, C. F. 2005. Basement Architecture and Sedimentary Fill of the North Makassar Straits Basin. *Proceedings Indonesian Petroleum Association 30th Annual Convention and Exhibition,* August 2005.
[18] Pubellier, M., and Morley, C. K. 2013. The Basins of Sundaland (SE Asia): Evolution and Boundary Conditions. *Journal of Marine and Petroleum Geology*. 58: 555-578. https://doi.org/10.1016/j.marpetgeo.2013.11.019.
[19] Advokaat, E. L., Marshall, N. T., Li, S., Spakman, W., Krijgsman, W., and van Hinsbergen, D. J. J. 2018. Cenozoic Rotation History of Borneo and Sundaland, SE Asia Revealed by Paleomagnetism, Seismic Tomography, and Kinematic Reconstruction. *Tectonics.* July 2018: 1-27. https://doi.org/10.1029/2018TC005010.
[20] Saller, A. H., and Vijaya, S. 2002. Depositional and Diagenetic History of the Kerendan Carbonate Platform, Oligocene, Central Kalimantan, *Indonesia. Journal of Petroleum Geology*. 25(2): 123-150. https://doi.org/10.1111/j.1747-5457.2002.tb00001.x.
[21] Morley, J. M., Morley, H. P., and Swiecicki, T. 2016. Mio-Pliocene Palaeogeography, Uplands and River Systems of the Sunda Region based on Mapping within a Framework of VIM Deposi-tional Cycles. *Proceedings Indonesian Petroleum Association 40th Annual Convention and Exhibition,* May 2016.
[22] McClay, K., Dooley, T., Ferguson, A., and Poblet, J. 2000. Tectonic Evolution of the Sanga Sanga Block, Mahakam Delta, Kalimantan, Indonesia. *The American Association of Petroleum Geologists (AAPG) Bulletin.* 84(6): 765-786. https://doi.org/10.1306/A96733EC-1738-11D7-8645000102C1865D.
[23] Moss, S. J., Chambers, J., Cloke, I., Satria, D., Ali, J. R., Baker, S., Milsom, J., and Carter. 1997. New Observation on the Sedimentary and Tectonic Evolution of the Tertiary Kutai Basin, East Kalimantan. In Fraser, A. J., Matthews, S. J., and Murphy, R. W. (Eds.). *Petroleum Geology of Southeast Asia. Geological Society Special Publication.* 126: 395-416. https://doi.org/10.1144/GSL.SP.1997.126.01.24.
[24] Wilson, M. E. J. and Moss, S. J. 1999. Cenozoic Palaeogeographic Evolution of Sulawesi and Borneo. *Palaeogeography, Palaeoclimatology, Palaeoecology*. 145: 303-337. Elsevier Science B.V. https://doi.org/10.1016/S0031-0182(98)00127-8.
[25] Harishidayat, D., Al-Shuhail, A., Randazzo, G., Lanza, S., Muzirafuti, A. 2022. Reconstruction of Land and Marine Features by Seismic and Surface Geomorphology Techniques. *Journals of Applied Sciences*. 12(19). https://doi.org/10.3390/app12199611.
[26] Morley, R. J., Hasan, S. S., Morley, H. P., Jais, J. H. M., Mansor, A., Aripin, M. R., Nordin, M. H., Rohaizar, M. H. 2021. Sequence Biostratigraphic Framework for the Oligocene to Pliocene of Malaysia: High-frequency Depositional Cycles Driven by Polar Glaciation. *Palaeogeography, Palaeoclimatology, Palaeoecology*. 561(1 January 2021): 110058. https://doi.org/10.1016/j.palaeo.2020.110058.
[27] van Wagoner, J. C., Posamentier, H. W., Mitchum, R. M., Vail, P. R., Sarg, J. F., Loutit, T. S., and Hardenbol, J. 1988. An Overview of the Fundamentals of Sequence Stratigraphy and Key Definitions. In Wilgus, C. K., Hastings, B. S., Posamentier, H. W., Van Wagoner, J. C., Ross, C. A., and Kendall, C.G.St.C. (Eds.). Sea Level Changes: An Integrated Approach. *SEPM Special Publication*. 42: 39-45. https://doi.org/10.2110/pec.88.01.0039.
[28] Posamentier, H. W. 2004. Seismic Geomorphology: imaging Elements of Depositional Systems from Shelf to Deep Basin using 3D Seismic Data: Implications for Exploration and Development, in 3D Seismic Technology: Applications to the Exploration of Sedimentary Basins. In Cartwright, R. J. *et al*. (Editors). 2004. *Geological Society, London, Memoirs*. 29: 11-24. https://doi.org/10.1144/GSL.MEM.2004.029.01.02.
[29] Dayong, V., A. 2018. Geochemistry and Mineralogy of Clastic Sediments of Tukau Formation: Implications on Provenance and Tectonic Setting. Thesis Degree of Master of Philosophy (Geology). Faculty of Engineering and Science, Curtin University, May 2018. 1-142. Unpublished.
[30] Ibrahim, A. M., Alshami, A., S., Abayazeed, S., D., Saadawy, D. A. 2019. Petrography, Paleoenvironment and Diagenetic Impact on Chemical Composition of Paleozoic Sandstones, Southwestern Sinai, Egypt. *Annals Geol. Surv. Egypt*. 127-149.